Available online at www.sciencedirect.com

ScienceDirect

IFAC PapersOnline CONFERENCE PAPER ARCHIVE

IFAC PapersOnLine 55-37 (2022) 752–757

Experimental Parameterization of a Model of Hypoxia Dynamics in Yorkshire Swine ⋆

Sam Wood * **Annina Commins** * **Mahsa Doosthosseini** **
Warren Naselsky *** **Melissa Culligan** **** **Kevin Aroom** †
Majid Aroom † **Behzad Kadkhodaeielyaderani** ‡ **Yejin Moon** ‡
Joshua Leibowitz *** **Shelby Stewart** § **Miao Yu** |
Joseph Friedberg ‡‡ **Jin-Oh Hahn** | **Hosam K. Fathy** |

* *B.S. in Mechanical Eng., Univ. of Maryland, College Park (UMCP).*
** *Postdoctoral fellow, UMCP.*
*** *Resident physician, Univ. of Maryland School of Medicine (UMSOM).*
**** *Ph.D. student, University of Maryland School of Nursing.*
† *Engineering researcher/faculty specialist, UMCP.*
‡ *Ph.D. student in Mechanical Engineering, UMCP.*
§ *Faculty member and thoracic surgeon, UMSOM.*
| *Mechanical engineering faculty member, UMCP.*
‡‡ *Thoracic Surgeon, Temple University.*

Abstract: This paper estimates the parameters of a model of hypoxia in large animals (specifically, Yorkshire swine) from experimental data. The paper adopts a simple, control-oriented model of oxygen transport and consumption dynamics. The model uses three state variables to represent oxygen concentrations and/or partial pressures in the animal's alveolar, arterial, and venous compartments. Hypoxia is induced in a laboratory animal by placing the animal on mechanical ventilation and reducing the fraction of inspired oxygen. The resulting dataset is used for the optimal estimation of key parameters governing the animal's oxygen transport, oxygen consumption, and hemoglobin dissociation. In this nonlinear system identification exercise, the optimization objective is a weighted sum of the mean square errors in predicting *(i)* blood oxygen saturation and *(ii)* end-tidal oxygen fraction. The resulting model fits the experimental hypoxia data reasonably well, and is intended as a baseline for ongoing research on the treatment of respiratory failure.

Keywords: Five to ten keywords, preferably chosen from the IFAC keyword list.

1. INTRODUCTION

This paper examines the problem of utilizing experimental data to identify simple, control-oriented, multi-compartment models of the dynamics of hypoxia in large animal models, such as Yorkshire swine. Such models can potentially provide insights into the underlying dynamics of hypoxia. Moreover, one can potentially use these models as baseline "digital twins" for assessing and optimizing different treatment modalities for respiratory failure.

The need for innovative treatments of respiratory failure is directly tied to its growing prevalence and cost. Even prior to the COVID-19 pandemic, for instance, Kempker et al. (2020) found an 83% increase in the per-capita incidence of respiratory failure-related hospitalizations in the United States between 2002-2017. This increase translated into an estimated 1,146,195 hospital discharges in 2017 with procedural codes associated with invasive mechanical ventilation, non-invasive mechanical ventilation, temporal tracheostomy, or extra-corporeal membrane oxygenation, with an average hospital stay of 10.5 days and an average hospitalization cost of $158,443.

Respiratory failure is typically treated using positive pressure mechanical ventilation, where the patient's airway is intubated to enable the supply of oxygen-rich inhaled gas at elevated pressures. Unfortunately, mechanical ventilation comes with the risk of ventilator-induced lung injury, or VILI (Lionetti et al. (2005)). This has the potential to trigger a positive feedback loop, where VILI creates a need for increasing ventilator pressures, but these pressures in turn exacerbate VILI, until mechanical ventilation no longer provides sufficient support to the patient. Once a patient exceeds the support achievable through mechanical ventilation alone, the only remaining treatment option is extra-corporeal membrane oxygenation (ECMO), where blood is drawn from the patient, oxygenated, then returned to the patient's bloodstream. Unfortunately, ECMO is a costly treatment that requires

⋆ This research was supported by NSF CMMI EAGER and NSF GCR awards (award numbers: CMMI#2031251, CMMI#2031245, and OIA#2121110) to Dr.s Joseph S. Friedberg, Jin-Oh Hahn, and Hosam K. Fathy (corresponding author, email: hfathy@umd.edu). The authors gratefully acknowledge this support. Animal experiments were conducted with Institutional Animal Care and Use Committtee (IACUC) approval from UMSOM (IACUC #0121006).

10.1016/j.ifacol.2022.11.272

constant monitoring by specialized medical professionals. Moreover, there are significant risks and contraindications that cause ECMO to not be available for many patient populations (Murphy et al. (2015)).

The research in this paper is motivated by the "third lung" concept - an additional potential treatment option for respiratory failure, beyond mechanical ventilation and ECMO. The main idea behind the third lung treatment is to perfuse (i.e., circulate) an oxygen-rich fluid through a patient's abdomen. Such perfusion has the potential to facilitate the diffusion-based transport of oxygen through the peritoneum, the highly vascularized lining of the abdominal cavity, and into the bloodstream. This potentially allows the abdomen to serve as a "third lung", similar to its role as a "third kidney" in peritoneal dialysis.

Different oxygen carriers can be used for peritoneal oxygenation. Perfluorocarbons (PFCs) are particularly appealing because of their extraordinarily high oxygen and carbon dioxide carrying capacities. Thanks to these properties, there is an extensive existing literature on liquid breathing: a medical intervention where oxygenated PFCs are circulated through the lungs to facilitate gas exchange. Examples of studies in this literature include work by Voelker et al. (2021), Sarkar et al. (2014), Staffey et al. (2008), Wolfson and Shaffer (2005), Hirschl et al. (2002), and Leach et al. (1996). The literature also presents multiple studies of the peritoneal or enteral perfusion of oxygenated liquids, including PFCs. Studies by Klein et al. (1986) and Carr et al. (2006), for instance, show that the peritoneal perfusion of oxygenated perfluorocarbons has the potential to serve as a supplementary gas exchange mechanism in both Wistar rats and Yorkshire swine, respectively. Moreover, research by Okabe et al. (2021) and Feshitan et al. (2014) proposes either the enteral perfusion of oxygenated PFCs or the peritoneal perfusion of phospholipid-coated oxygen microbubbles as potential alternatives to the peritoneal perfusion of oxygenated PFCs. Finally, ongoing research by the investigators presents a mechatronic perfusion setup for experiments on the third lung concept in large laboratory animals such as Yorkshire swine (Doosthosseini et al. (2022)).

The main goal of this paper is to use the experimental data generated by the above mechatronic third lung setup to identify a simple dynamic model of hypoxia in Yorkshire swine. The paper focuses specifically on modeling the dynamic impact of changes in the fraction of inspired oxygen, FiO_2, on the resulting partial pressures of oxygen in the alveolar, arterial, and venous compartments. Two potential metrics for model parameterization and/or validation are the ability to predict the end-tidal oxygen fraction and the percent arterial oxygen saturation. Both metrics are used in this work, as part of a multi-objective nonlinear system identification effort. The ultimate intent of this paper's model is to serve as a baseline for assessing the dynamic impact of perfusion on hypoxia in future research.

There is an extensive existing literature on the modeling of respiratory system dynamics. Examples of work in this literature include studies by Ben-Tal and Tawhai (2013), Lu et al. (2003), Whiteley et al. (2003), Ursino et al. (2001), Batzel and Tran (2000), Chiari et al. (1997), and Khoo et al. (1982). The focus in most of this literature is on human respiratory dynamics. This focus is strongly justified from the ultimate perspective of clinical applicability. However, the model-based analysis of animal experiments on ventilation concepts such as the "third lung" requires experimentally-parameterized models of hypoxia dynamics in the corresponding laboratory animals. This explains the focus of this paper on the experimental parameterization of the dynamics of hypoxia in Yorkshire swine.

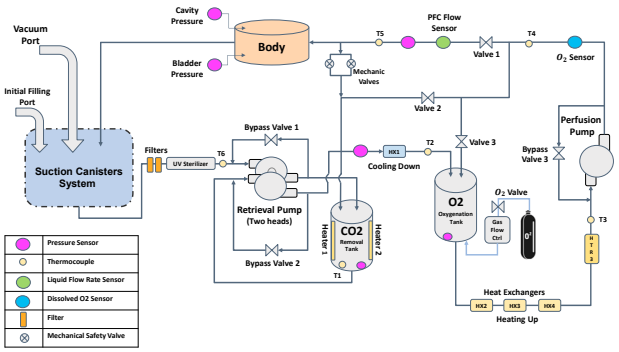

Fig. 1. Schematic of the third lung setup

Seven animal experiments have been conducted to date using the third lung setup developed by Doosthosseini et al. (2022), all of them using adult Yorkshire swine. This paper focuses specifically on the second animal experiment. Hypoxia was induced in this experiment through a reduction in the fraction of inspired oxygen, FiO_2, first without PFC perfusion then with PFC perfusion. The contribution of this paper is to model and parameterize the dynamics of hypoxia without perfusion, with the ultimate intent of using the resulting model as a baseline for examining the impact of perfusion on hypoxia in future research.

The remainder of this paper is organized as follows. Section 2 summarizes the design of the perfusion setup used in the above animal experiment. Section 3 then summarizes the proposed model of animal hypoxia. Section 4 presents the experimental data used for parameterizing this model, the formulation of the optimal parameterization problem, and the parameterization results. Finally, Section 5 summarizes the paper's lessons and conclusions.

2. EXPERIMENTAL SETUP

Fig. 1 is a high-level schematic of the "third lung" perfusion setup used in this work, and described in depth in a companion paper by Doosthosseini et al. (2022). The setup uses an AVS mechanical ventilator connected to a Penlon monitor to adjust respiratory control input variables such as the fraction of inspired oxygen and minute ventilation rate. A Capnomac capgnograph is used for measuring respiratory response (i.e., output) variables such as the end-tidal oxygen fraction. Percent artertial oxygen saturation is measured by a pulse oximetry probe that can be attached to either the animal's tongue or ear, and is connected to a Nellcor pulse oximeter. Additional physiological variables, including heart rate, are read by a

Tram-Rac patient monitor. Measurements from all of these medical instruments are communicated either directly (as analog voltage signals) or indirectly (as RS-232 signals that are read by a set of Arduino/Teensy boards then repackaged into a single RS-232 data stream) into a dSpace MicroLabBox-II data acquisition board. When perfusion experiments are conducted, two peristaltic pumps are used for pumping the PFC flow returning from the animal through a sequence of canisters used for fluid CO_2 removal, oxygenation, and heating/cooling. Several control loops, most of them employing PID control with saturation limits plus anti-windup control, are used for controlling the volumetric flowrate, pressure, temperature, and oxygenation level with which oxygenated PFC is supplied to the animal. Preparation for perfusion involves the surgical intubation of the animal's abdomen with $12mm$ diameter (i.e., 36-French) inflow and outflow cannulas connected to the above setup.

A typical hypoxia experiment proceeds as follows. The laboratory animal is first anesthesized and placed on mechanical ventilation. Next, the fraction of inspired oxyen is reduced to induce hypoxia, then increased to facilitate recovery from hypoxia without perfusion. Finally, the fraction of inspired oxygen is reduced again to induce hypoxia, and the perfusion of oxygenated PFC commences, with the goal of quantifying the impact of this perfusion on the dynamics of hypoxia. A similar sequence of steps is used for examining the dynamics of hypercarbia, with the main distinction being the use or reductions in minute ventilation (as opposed to inspired oxygen) to induce hypercarbia.

3. HYPOXIA MODEL

The goal of this paper is to fit the following third-order state-space model to the experimentally observed dynamics of hypoxia:

$$\begin{aligned} \dot{x}_1 &= \frac{u_1}{60V_L}(u_2 - x_1) + k_1(x_2 - f_d(x_1)) \\ \dot{x}_2 &= k_2(f_d(x_1) - x_2) + k_3(x_3 - x_2) \\ \dot{x}_3 &= k_4(x_2 - x_3) - w \\ y_1 &= x_2 \\ y_2 &= f_d(x_1) \end{aligned} \tag{1}$$

In the above state-space model, t denotes time in seconds. The model is a three-compartment representation of gas transport dynamics, with the three compartments being the alveoli, arteries, and veins. As a result, the model contains three state variables, namely: $x_1(t)$, the alveolar partial pressure of oxygen in $mmHg$, $x_2(t)$, the arterial percentage oxygen saturation (dimensionless), and $x_3(t)$, the venous percentage oxygen saturation (dimensionless). There are two inputs to the model, namely, $u_1(t)$, the animal respiration rate in liters per minute, and $u_2(t)$, the partial pressure of inspired O_2, in $mmHg$. Finally, the model has two measured output variables, namely, $y_1(t)$, representing percentage pulse oximetry, and $y_2(t)$, representing the end-tidal fraction of oxygen (expressed as a percentage). The term $u_1(u_2 - x_1)/60V_L$ represents the advective transport of oxygen into and out of the alveolar (or lung) compartment, with V_L representing total effective lung volume (including dead space). The coefficients $k_{1,2,3,4}$ represent a linearized idealization of gas transport between the three compartments. Three of these coefficients have units of sec^{-1}, with k_1 being in $mmHg.sec^{-1}$ per percent O_2 saturation. Possible differences in the effective volumes of the three compartments imply that the lumped parameters k_1 and k_3 do not necessarily have to equal k_2 and k_4, respectively. The term w is a constant disturbance term representing the impact of metabolism on venous oxygen saturation. Specifically, one can construe w as the rate at which metabolism alone contributes to the depletion of percentage venous oxygen saturation, in units of percent venous saturation reduction per second. Finally, the function f_d is a mathematical representation of the hemoglobin dissociation curve, and is assumed to be governed by the classical Hill equation:

$$f_d(x_1) = 100\frac{\left(\frac{x_1}{P_o}\right)^r}{1 + \left(\frac{x_1}{P_o}\right)^r} \tag{2}$$

,

where r is a dimensionless coefficient and P_o is the partial pressure of O_2, in $mmHg$, corresponding to 50% oxygen saturation.

The above model makes a number of approximations in pursuit of simplicity, computational efficiency, and ease of parameterization. Consistent with the multi-compartment modeling literature, gas concentration and/or partial pressure is assumed to be spatially uniform in each compartment, and the outflow from each compartment (e.g., end-tidal oxygen) is approximated as having the same composition as the gas within the compartment. Gas exchange between the lungs and the ambient environment is approximated as a continuous process, as opposed to modeling the instantaneous inflow and outflow associated with inhalation and exhalation, respectively: a simplification that allows the volume V_L to be approximated as constant. A single compartment is used for representing the lungs, as opposed to a sequence of multiple compartments representing different spaces within the lungs. Inter-compartment transport dynamics are approximated as linear dynamics, and the associated transport time delays are neglected. The model focuses on physical gas transport, as opposed to the physiological feedback mechanisms influencing this transport. Finally, the model approximates metabolic oxygen consumption as constant, independent of the animal's state of hypoxia or hypercarbia, and neglects the impact of blood pH (due to factors such as hypercarbia) on the hemoglobin dissociation curve. Collectively, these assumptions emphasize simplicity and ease of parameterization, furnishing a control-oriented model that nevertheless captures the dynamics of hypoxia reasonably well, as shown in the next section.

4. SYSTEM IDENTIFICATION APPROACH AND RESULTS

Fig. 2 plots the fraction of inspired oxygen as a function of time (as a percentage) during the hypoxia trial examined in this paper. Inspired oxygen was cut approximately by half during this trial. As shown in Fig. 3, this corresponded to a relatively steady minute ventilation rate, increasing

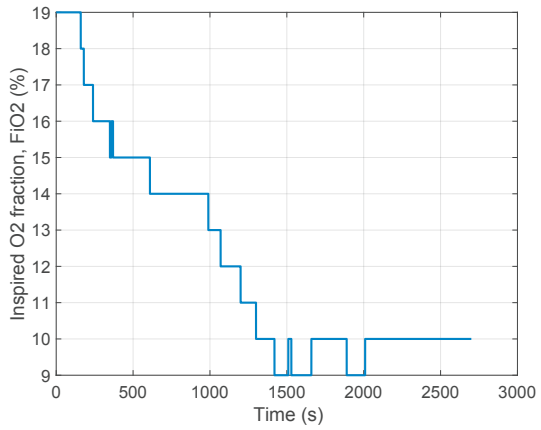

Fig. 2. Inspired oxygen input trajectory

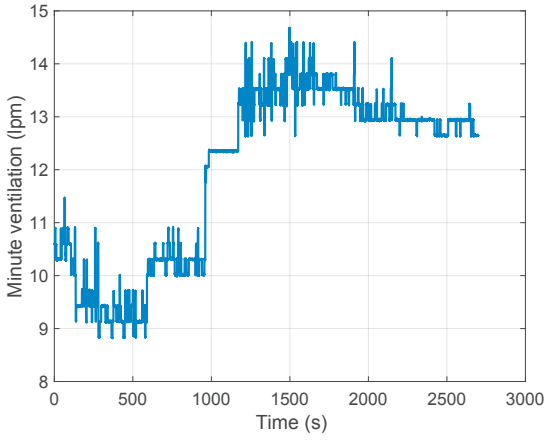

Fig. 3. Minute ventilation input trajectory

only slightly during the hypoxia trial. Nonlinear system identification was used for fitting the dynamics of the resulting hypoxia. Specifically, an optimization problem was solved where:

- The optimization variables were: the initial conditions for the three state variables, the effective lung volume V_L, the transport coefficients $k_{1,2,3,4}$, the metabolic oxygen depletion rate w, and the constants, r and P_o, in the Hill equation.
- Simple bounds were imposed on all of the above optimization variables. With the exception of the upper bound of 100% on the initial arterial and venous oxygen saturation levels, none of the optimization variables were close to their bounds at the optimum.
- The main optimization constraint was the satisfaction of the state-space dynamics, numerically integrated in time using the first-order forward Euler algorithm, with a $0.25sec$ time step.
- The optimization objective was to minimize the summation of the squared errors in predicting percentage pulse oximetry plus a Pareto weight times the summation of the squared errors in predicting the end-tidal oxygen partial pressure, in $mmHg$. The Pareto weight in this case had a value of $0.05\%mmHg^{-1}$. Because end-tidal O_2 measurements were only available from the capnograph every 10 seconds, the estimate of y_2 was also sampled once every 10 seconds prior to the computation of the second term in the above Pareto objective.

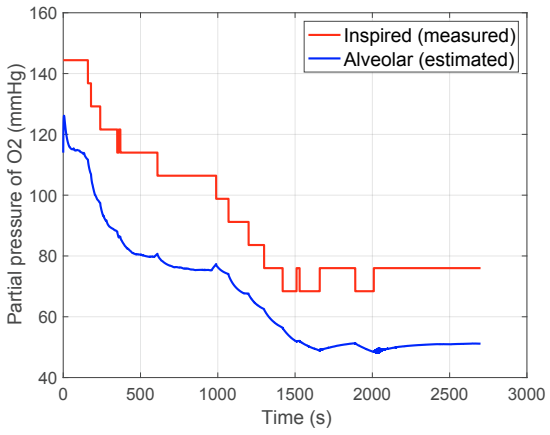

Fig. 4. Respiratory oxygen trajectories

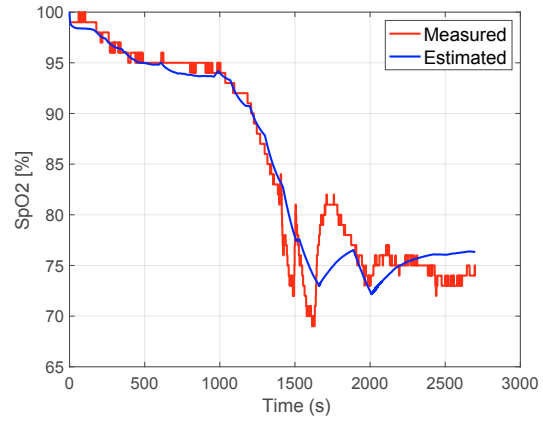

Fig. 5. Pulse oximetry trajectories

Fig. 4 plots the predicted partial pressure of alveolar O_2 versus the measured partial pressure of inspired O_2. A reasonable gradient is predicted by the model, consistent with the assumption that the latter quantity represents an approximation of the end-tidal partial O_2 pressure. Fig. 5 provides the main model validation result in this paper, showing that the fitted model does a reasonable job capturing the dynamics of pulse oximetry during hypoxia. An important secondary validation result is shown in Fig. 6, highlighting the model's success in capturing the dynamics of end-tidal O_2 accurately, even with the low Pareto weight and infrequent sampling associated with this signal. The estimated end-tida O_2 trajectory in this figure is sampled from the proposed model at the same sampling instant as the measurement data, to ensure consistent sampling when comparing the two signals. Finally, Fig. 7 shows the hemoglobin dissociation curve estimate associated with the identified model. This curve is reasonably consistent with the literature: an important and encouraging result.

The following parameter estimates were obtained from the above system identification exercise. Effective lung volume had a physiologically plausible estimate of $V_L =$

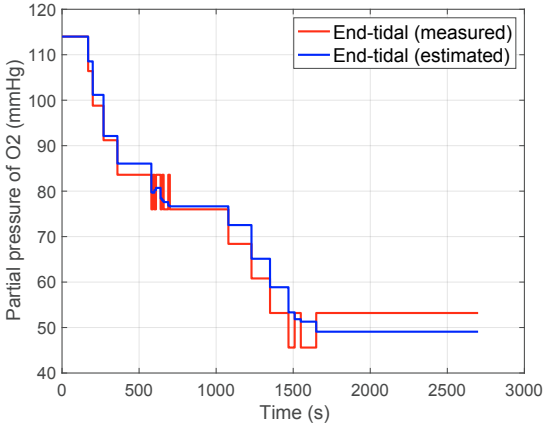

Fig. 6. End-tidal oxygen trajectories

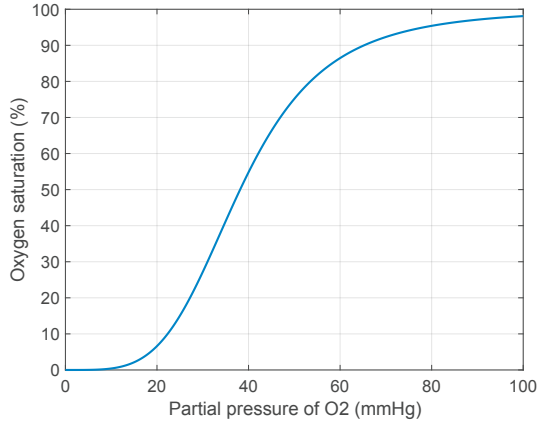

Fig. 7. Estimated hemoglobin dissociation curve

$2.19L$. Two of the transport constants had large estimates, namely, $k_1 = 4.54mmHg.s^{-1}$ per percent O_2 saturation and $k_4 = 4.60s^{-1}$, reflecting a potential need for model reduction to prevent over-fitting and/or structural identifiability issues. The other two transport constants had more physiologically plausible values of $k_2 = 0.369s^{-1}$ and $k_3 = 0.173s^{-1}$. The metabolic consumption constant had a physiologically plausible estimate of $w = 1.30\%s^{-1}$. The initial estimate of x_1 was $114mmHg$, which is very reasonable. However, the initial esimates of x_2 and x_3 were both very close, with values of 99.997% and 99.933%, respectively. This is a reasonable range for arterial pulse oximetry, but not venous oximetry, indicating (once again) the need for further model reduction to overcome potential overfitting and/or parameter identifiability issues. Finally, the coefficients of the hemoglobin dissociation curve had physiologically plausible estimates of $r = 4.10$ and $P_o = 38.2mmHg$, respectively. One consequence of the above parameter values is that under steady state equilibrium conditions, the metabolic oxygen depletion rate w is equivalent to an inhalation-based oxygen intake rate of $104mL.min^{-1}$, a value that is at the low end of physiologically plausible Yorkshire swine metabolic oxygen consumption rates.

5. DISCUSSION AND CONCLUSIONS

The above model parameterization results reveal three important insights. First, the proposed oxygen transport model is reasonably accurate in capturing the dynamics of both pulse oximetry and end-tidal oxygen fraction during hypoxia. This is an encouraging result, particularly in light of potential future work on the use of such a model as a baseline for the study of the impact of peritoneal PFC perfusion on these dynamics. Second, the fact that the model has reasonable prediction accuracy in the presence of multiple underlying simplifying assumptions suggests that the use of simple, control-oriented models for studying hypoxia is a reasonable first step towards more sophisticated hypoxia models. Third, the excessively fast transport coefficients estimated by the model, particularly when viewed in light of the sampling rates provided by instruments such as the Capnomac, suggest that the model's parameters are likely to suffer from identifiability issues. Exploring both these identifiability issues and their remedies, including model reduction, is an important topic for future research. The dynamics of venous blood oxygen saturation, in particular, are coupled to arterial saturation dynamics through an excessively fast time constant of $k_4.60s^{-1}$, with very similar (nearly boundary-optimal) initial estimates for these saturation levels. This suggests that the identifiability of the venous dynamics (i.e., the dynamics of $x_3(t)$), in particular, may require significant further examination.

REFERENCES

Batzel, J.J. and Tran, H.T. (2000). Stability of the human respiratory control system i. analysis of a two-dimensional delay state-space model. *Journal of mathematical biology*, 41(1), 45–79.

Ben-Tal, A. and Tawhai, M.H. (2013). Integrative approaches for modeling regulation and function of the respiratory system. *Wiley Interdisciplinary Reviews: Systems Biology and Medicine*, 5(6), 687–699.

Carr, S.R., Cantor, J.P., Rao, A.S., Lakshman, T.V., Collins, J.E., and Friedberg, J.S. (2006). Peritoneal perfusion with oxygenated perfluorocarbon augments systemic oxygenation. *Chest*, 130(2), 402–411.

Chiari, L., Avanzolini, G., and Ursino, M. (1997). A comprehensive simulator of the human respiratory system: validation with experimental and simulated data. *Annals of biomedical engineering*, 25(6), 985–999.

Doosthosseini, M., Aroom, K.R., Aroom, M.R., Culligan, M., Naselsky, W., Thamire, C., Haslach, H.W., Roller, S.A., Hughen, J.R., Friedberg, J.S., et al. (2022). Monitoring, control system development, and experimental validation for a novel extrapulmonary respiratory support setup. *IEEE/ASME Transactions on Mechatronics*.

Feshitan, J.A., Legband, N.D., Borden, M.A., and Terry, B.S. (2014). Systemic oxygen delivery by peritoneal perfusion of oxygen microbubbles. *Biomaterials*, 35(9), 2600–2606.

Hirschl, R.B., Croce, M., Gore, D., Wiedemann, H., Davis, K., Zwischenberger, J., and Bartlett, R.H. (2002). Prospective, randomized, controlled pilot study of partial liquid ventilation in adult acute respiratory distress

syndrome. *American journal of respiratory and critical care medicine*, 165(6), 781–787.

Kempker, J.A., Abril, M.K., Chen, Y., Kramer, M.R., Waller, L.A., and Martin, G.S. (2020). The epidemiology of respiratory failure in the united states 2002–2017: A serial cross-sectional study. *Critical Care Explorations*, 2(6).

Khoo, M., Kronauer, R.E., Strohl, K.P., and Slutsky, A.S. (1982). Factors inducing periodic breathing in humans: a general model. *Journal of applied physiology*, 53(3), 644–659.

Klein, J., Faithfull, N.S., Salt, P.J., and Trouwborst, A. (1986). Transperitoneal oxygenation with fluorocarbons. *Anesthesia and analgesia*, 65(7), 734–738.

Leach, C.L., Greenspan, J.S., Rubenstein, S.D., Shaffer, T.H., Wolfson, M.R., Jackson, J.C., DeLemos, R., and Fuhrman, B.P. (1996). Partial liquid ventilation with perflubron in premature infants with severe respiratory distress syndrome. *New England Journal of Medicine*, 335(11), 761–767.

Lionetti, V., Recchia, F.A., and Ranieri, V.M. (2005). Overview of ventilator-induced lung injury mechanisms. *Current opinion in critical care*, 11(1), 82–86.

Lu, K., Clark Jr, J., Ghorbel, F., Ware, D., Zwischenberger, J., and Bidani, A. (2003). Whole-body gas exchange in human predicted by a cardiopulmonary model. *Cardiovascular Engineering: An International Journal*, 3(1), 1–19.

Murphy, D.A., Hockings, L.E., Andrews, R.K., Aubron, C., Gardiner, E.E., Pellegrino, V.A., and Davis, A.K. (2015). Extracorporeal membrane oxygenation—hemostatic complications. *Transfusion medicine reviews*, 29(2), 90–101.

Okabe, R., Chen-Yoshikawa, T.F., Yoneyama, Y., Yokoyama, Y., Tanaka, S., Yoshizawa, A., Thompson, W.L., Kannan, G., Kobayashi, E., Date, H., et al. (2021). Mammalian enteral ventilation ameliorates respiratory failure. *Med*, 2(6), 773–783.

Sarkar, S., Paswan, A., and Prakas, S. (2014). Liquid ventilation. *Anesthesia, essays and researches*, 8(3), 277.

Staffey, K.S., Dendi, R., Brooks, L.A., Pretorius, A.M., Ackermann, L.W., Zamba, K., Dickson, E., and Kerber, R.E. (2008). Liquid ventilation with perfluorocarbons facilitates resumption of spontaneous circulation in a swine cardiac arrest model. *Resuscitation*, 78(1), 77–84.

Ursino, M., Magosso, E., and Avanzolini, G. (2001). An integrated model of the human ventilatory control system: the response to hypoxia. *Clinical Physiology*, 21(4), 465–477.

Voelker, M.T., Laudi, S., Henkelmann, J., and Bercker, S. (2021). Ecmo and perfluorocarbon in a therapy refractory case of acute respiratory distress syndrome. *The Annals of Thoracic Surgery*.

Whiteley, J.P., Gavaghan, D.J., and Hahn, C.E. (2003). Mathematical modelling of pulmonary gas transport. *Journal of mathematical biology*, 47(1), 79–99.

Wolfson, M.R. and Shaffer, T.H. (2005). Pulmonary applications of perfluorochemical liquids: ventilation and beyond. *Paediatric respiratory reviews*, 6(2), 117–127.